Applied Catalysis B: Environmental 84 (2008) 389–392

Contents lists available at ScienceDirect

Applied Catalysis B: Environmental

journal homepage: www.elsevier.com/locate/apcatb

Review

Enhanced photocatalytic activity of Au-buffered TiO_2 thin films prepared by radio frequency magnetron sputtering

Jong Min Jung [a], Mingsong Wang [b], Eui Jung Kim [b], Chinho Park [c], Sung Hong Hahn [a,*]

[a] Department of Physics, University of Ulsan, Ulsan 680-749, South Korea
[b] Department of Chemical Engineering, University of Ulsan, Ulsan 680-749, South Korea
[c] School of Chemical Engineering and Technology, Yeungnam University, Gyeongsan 712-749, South Korea

ARTICLE INFO

Article history:
Received 15 January 2008
Received in revised form 10 April 2008
Accepted 16 April 2008
Available online 25 April 2008

Keywords:
Sputtering method
TiO_2 thin films
Au-buffer layer
Photocatalytic activity

ABSTRACT

Au-buffered TiO_2 thin films have been prepared by radio frequency magnetron sputtering method. The structural and morphological properties of the thin films were characterized by X-ray diffraction, scanning electron microscopy, and atomic force microscopy. The photocatalytic activity of the samples was evaluated by the photodecomposition of methylene blue. The Au-buffer thin layer placed between the TiO_2 thin films significantly enhanced photocatalytic activity by 50%. Annealing the Au-buffered TiO_2 thin film at 600 °C decreased the film roughness, but it increased the surface area and anatase crystalline size, enhancing the photocatalytic activity.

Contents

1. Introduction

Titanium dioxide (TiO_2) has very effective photodegradation activity for organic pollutants in water and air under the irradiation of ultraviolet (UV) light due to its high photosensitivity, non-toxic nature, large band-gap and stability [1–4]. The photocatalytic activity of TiO_2 can be influenced by its crystal structure, surface area, size distribution, and porosity [5]. When TiO_2 catalysts are subject to UV irradiation with photons of energy equal to or higher than their band-gap, electron–hole pairs are generated and induce the formation of reactive species such as $^{\bullet}OH$ and $^{\bullet}O_2^-$ that are directly involved in the oxidation processes leading to degradation of pollutants [6–12]. The efficiency of TiO_2 photocatalyst systems depends directly on the recombination rate of the generated electron–hole pairs [12]. Moreover, an increase in photocatalytic efficiency has been observed in the metal–TiO_2 composites owing to a reduction in electron–hole recombination rate [5,11–13]. The photocatalytic efficiency of metal–TiO_2 composite nanosystems depends on both the metal loading amount and preparation route. Sakthivel et al. [5] reported that the photocatalyst efficiency depends on the dosage of Au, Pt, Pd. It was also reported that homogeneous distribution of Au nanoaggregates and Ag microgrid deposited on the TiO_2 surface improves the photocatalyst efficiency [14,15]. Due to the difference in the work functions of TiO_2, Au and Ag, conduction band electrons can be attracted by the metal particles, thus preventing electron–hole recombination. The electrons accumulated in the gold are consumed by reacting with oxygen. An increase in the amount

* Corresponding author. Tel.: +82 52 259 2330; fax: +82 52 259 1693.
E-mail address: shhahn@mail.ulsan.ac.kr (S.H. Hahn).

0926-3373/$ – see front matter © 2008 Elsevier B.V. All rights reserved.
doi:10.1016/j.apcatb.2008.04.020

of the doped metal lowers the photocatalyst efficiency. We present here a new method in order to solve this problem.

Recently, we have observed the enhanced photocatalytic efficiency of the Au/TiO_2 composite thin film prepared by radio frequency (RF) magnetron sputtering [16]. In this work, we have proposed a novel structure by placing an Au-buffer thin layer between TiO_2 thin films. The photocatalytic activity of the TiO_2 thin films was found to be markedly enhanced in the presence of the Au-buffer layer.

2. Experiments

Au-buffered TiO_2 thin films were deposited on quartz glass by using a RF magnetron sputtering system in a high vacuum reactor with three separate focal sources. The TiO_2 and Au target with a size of 5×10^{-2} m in diameter were powered by an RF generator at a frequency of 13.56 MHz. The TiO_2 ceramic target was prepared by sintering it in air at 1200 °C for 5 h. The base pressure of the chamber was 3.5×10^{-6} Torr. The deposition pressure was set at 1.0×10^{-2} Torr. The flow rate of Ar (99.99%) was controlled with a mass flow meter system. The optimum substrate-to-target distance was determined to be 150 mm. Before each run, the targets were pre-sputtered in argon for 10 min to clean the surface of the targets. The RF power for the TiO_2 and Au target was 200 and 20 W, respectively. Since it is hard to directly deposit an Au layer on the quartz substrate, we developed a TiO_2/Au/TiO_2 structure to prepare an Au-buffered TiO_2 thin films; a TiO_2 thin layer (ca. 50 nm in thickness) was first deposited on the quartz substrate, then an Au-buffer thin layer (ca. 10 nm in thickness) was deposited, and finally TiO_2 thin film of ca. 150 nm in thickness was deposited on the Au-buffer layer at room temperature. After the deposition, some samples were annealed in air at 600 °C for 1 h to form the anatase phase.

The photocatalytic properties of the prepared thin films were evaluated by measuring the photodecomposition of methylene blue ($C_{16}H_{18}N_3S$–Cl–$3H_2O$) in aqueous solution with an initial concentration of 1×10^{-5} mol/L. The samples with a size of 2 cm^2 were immersed in the dye solution in a tubular quartz reactor. The solution was vigorously stirred under irradiation of four surrounding 20 W-black-light lamps (wavelength = 352 nm). Photocatalytic degradation was monitored by measuring the absorption spectra of the solution at λ_{max} = 664 nm.

The crystal phase of the samples was determined by X-ray diffraction (XRD, Philips PW3710) in the 2θ mode using monochromatic Cu Kα radiation at a grazing incidence ($\theta = 4°$). A scanning electron microscope (SEM, Hitachi S-4200) and atomic force microscope (AFM, Digital Instrument) were used to examine the morphologies of the thin films. The absorption spectra of the dye solution were measured by using an UV–vis spectrophotometer (HP 8453).

3. Results and discussion

Fig. 1 shows the XRD patterns of the as-deposited and 600 °C-annealed TiO_2 and Au-buffered TiO_2 thin films. Fig. 1a and b indicate that the as-deposited samples are amorphous. The anatase phase is formed post-annealing at 600 °C for 1 h (Fig. 1c and d). For Au-buffered TiO_2, the Au-buffer thin layer was identified by the diffraction peaks of (1 1 1) and (2 0 0) for cubic gold (Fig. 1b and d). Determined from the full width at half maximum (FWHM) of the TiO_2 (1 0 1) peak using the Scherrer formula ($d = 0.9\,\lambda/H\cos\theta$), the crystallite size of anatase in the 600 °C-annealed TiO_2 and Au-buffered TiO_2 thin films is 20.9 and 19.8 nm, respectively. Generally, TiO_2 has the anatase, rutile and brookite phase depending on the annealing temperature [16]. It is seen in Fig. 1

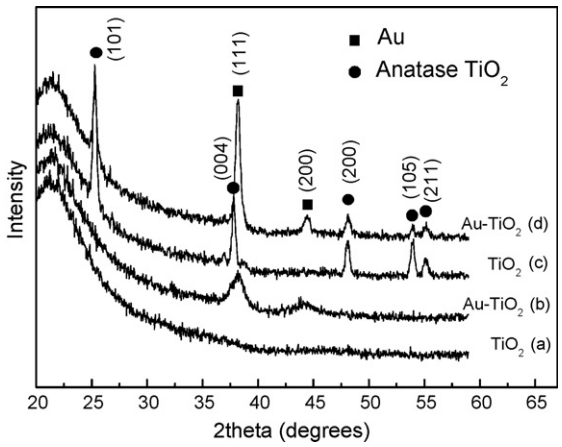

Fig. 1. XRD patterns of the as-deposited (a and b) and 600 °C-annealed (c and d) TiO_2 and Au-buffered TiO_2 thin films.

that post-annealing the samples at 600 °C for 1 h leads to formation of anatase TiO_2 that is the most favorable phase for the photocatalytic process. The diffraction peak at $2\varnothing = 38.4°$ was used to calculate the grain size of fcc Au of the as-deposited and 600 °C-annealed Au-buffered TiO_2 thin films. Fig. 2 shows the diffraction peak at $2\varnothing = 38.4°$ for the as-deposited Au-buffered TiO_2 thin films consisting of the anatase (0 0 4) and Au (1 1 1) peaks. The crystallite size of fcc Au of the as-deposited and 600 °C-annealed Au-buffered TiO_2 is found to be 6.4 nm and 9.5 nm, respectively.

Fig. 3 illustrates the UV–vis absorption spectra of TiO_2 and Au-buffered TiO_2 thin films. In general, the band-gap absorption edge of titania is located at $\lambda \leq 380$ nm. In the case of the Au-buffered TiO_2 thin films, an absorbance band appears in the 350–450 nm range. The absorbance band results from the plasmon resonance of metallic Au particles [17–19]. In metal nanoparticles of Au^0, Cu^0, and Ag^0, the plasmon absorption arises from the collective oscillations of the free conduction band electrons that are induced by the incident electromagnetic radiation.

Fig. 4 shows the SEM and AFM images of TiO_2, Au-buffered TiO_2 (b, e and h), and 600 °C-annealed Au-buffered TiO_2 thin films. The top-view SEM images illustrate that all films are homogeneous and crack-free (Fig. 4a–c). It is also seen in Fig. 4b that the secondary particles of TiO_2 in the films grow bigger in the presence of the

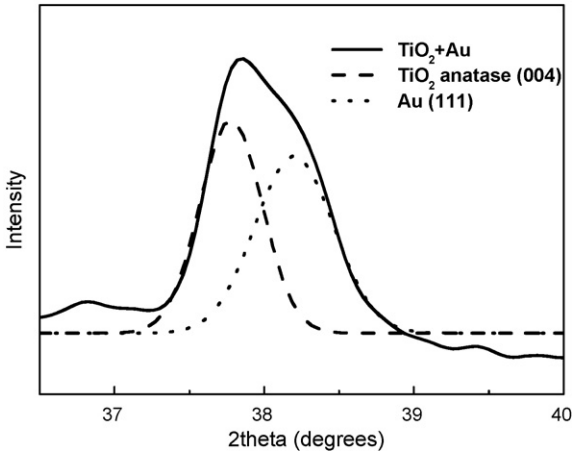

Fig. 2. The diffraction peak at $2\varnothing = 38.4°$ for the as-deposited Au-buffered TiO_2 thin films consisting of the anatase (0 0 4) and Au (1 1 1) crystal peaks.

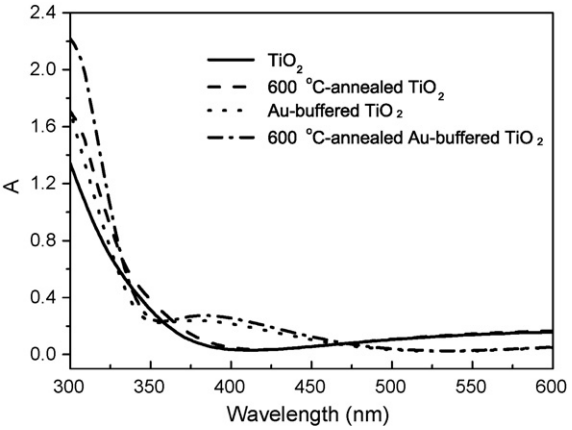

Fig. 3. UV–vis spectra of TiO_2 and Au-buffered TiO_2 thin films.

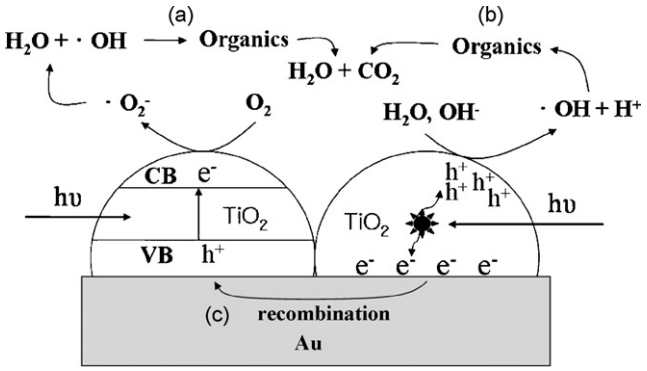

Fig. 5. Schematic illustration of photodegradation by Au-buffered TiO_2 thin films.

Au-buffer thin layer. The particle size of TiO_2 becomes even bigger post-annealing (Fig. 4c). The side-view SEM images clearly show the Au thin layer between the TiO_2 thin films for the Au-buffered samples (Fig. 4e and f). The thickness of the Au-buffer layer and top TiO_2 layer is ca. 10 and 150 nm, respectively. In Fig. 4g and h, the AFM images of the samples indicate that the roughness of thin films is increased by 36% to 1.48 nm in the presence of the Au-buffer layer. However, post-annealing the samples result in a decrease in film roughness to 0.83 nm (Fig. 4i).

The initial process for photocatalysis of organic compounds by TiO_2 is the generation of e^-–h^+ pairs in the TiO_2 particles after the absorption of a photon with energy equal to or higher than the band-gap of TiO_2 as sketched in Fig. 5a. The generated holes (h^+) react with H_2O and OH^- groups adsorbed on the surface of TiO_2 to produce hydroxyl radicals [20], and the electrons (e^-) are attracted to the metal buffer layer due to the difference in the work functions of TiO_2 and Au (Fig. 5b), thus preventing the e^-–h^+ recombination [21]. The electrons accumulated in the gold layer are consumed by two reactions. Firstly, the electrons accumulated in the Au layer reunite with the holes unable to react with the water. Secondly, the electrons are consumed by reuniting with the holes formed at the (a) process [14] (Fig. 5c). Organic compounds are completely decomposed into water and carbon dioxide by reacting with the produced hydroxyl radicals.

Fig. 6 shows the photocatalytic degradation of methylene blue for various samples. It is seen in Fig. 6 that the photolysis of the dye

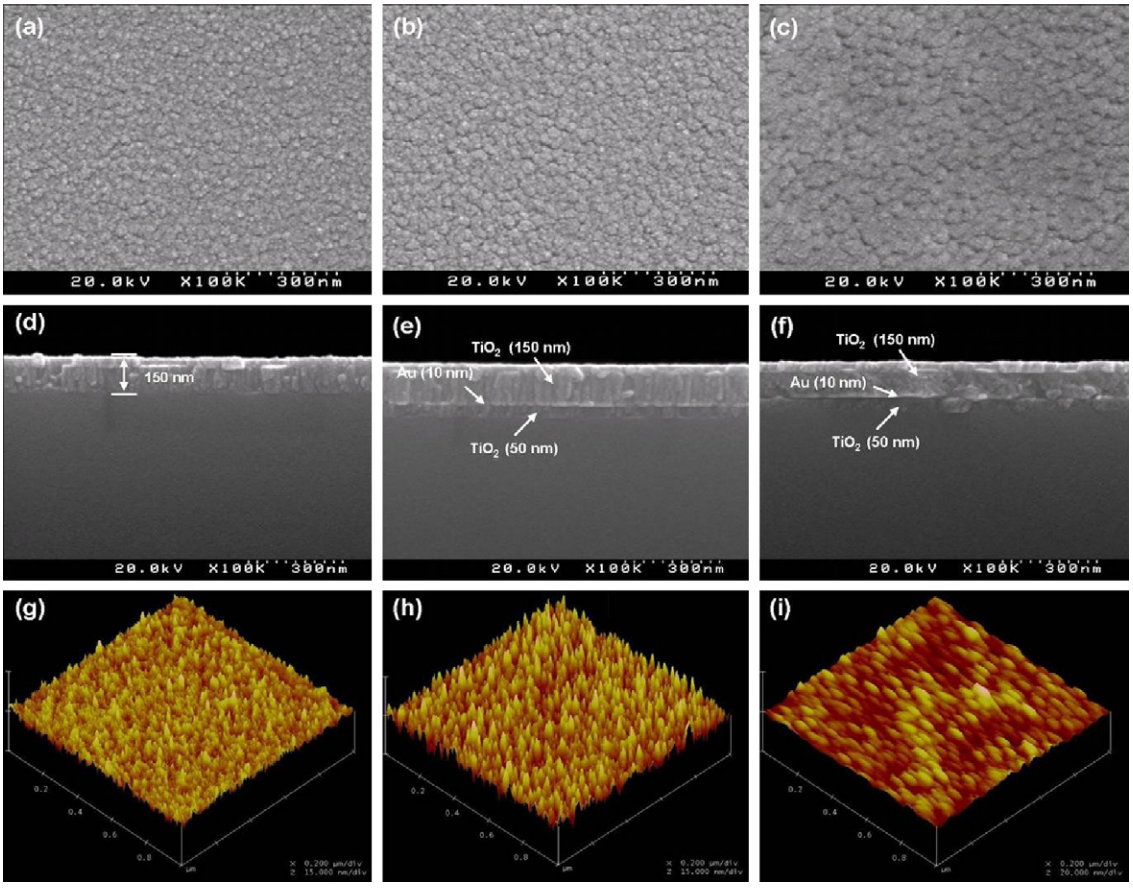

Fig. 4. SEM (a–f) and AFM (g–i) images of TiO_2 (a, d and g), Au-buffered TiO_2 (b, e and h), and 600 °C-annealed Au-buffered TiO_2 (c, f and i) thin films.

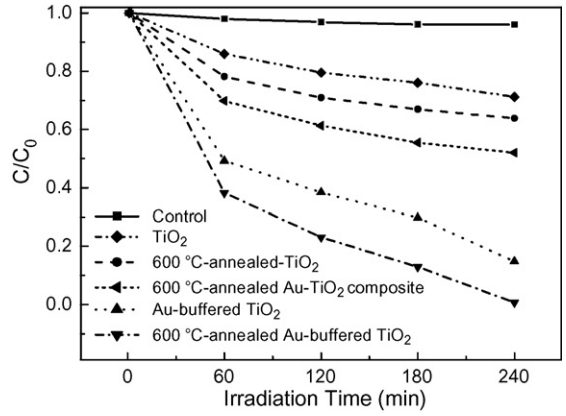

Fig. 6. Photodegradation of methylene blue as a function of irradiation time.

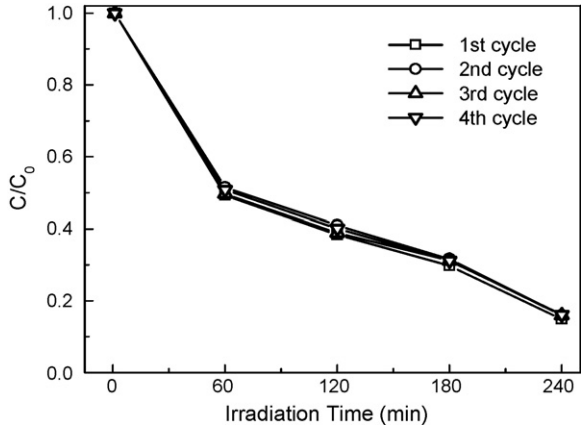

Fig. 7. Photoactivity of the as-deposited Au-buffered TiO_2 thin film after its repeated use.

solution by UV light is negligible in the absence of a photocatalyst. However, 30% of the dye is decomposed after 4 h for the as-deposited amorphous TiO_2 thin film. The efficiency of the photodegradation is enhanced post-annealing at 600 °C. In the case of the Au-TiO_2 composite (Au embedded in TiO_2) thin film catalyst [16], 50% of the dye solution is decomposed after 4 h UV irradiation. However, photocatalytic activity is markedly enhanced in the presence of the Au-buffer layer even though the as-deposited TiO_2 is amorphous. We believe that the Au-buffer layer inhibits the recombination of charge carriers by electron capture. Thus more holes are available to produce hydroxyl radicals enhancing the photodegradation. As is expected, 600 °C-annealed Au-buffered TiO_2 demonstrates the most efficient photocatalysis due to the anatase phase of TiO_2 and inhibited charge carrier recombination. It is worthy of noting that notwithstanding the decreased surface roughness from 1.48 to 0.83 nm the photocatalytic efficiency of the as-deposited Au-buffered TiO_2 is enhanced post-annealing. Tian et al. [22] reported that the film roughness depends on the annealing temperature. In their experiments, the film roughness was reduced after annealing at 600 °C but the surface area was increased, which is consistent with our results. This result suggests the anatase crystalline phase and surface area of TiO_2 plays a more important role in the photocatalytic process than the film roughness.

Fig. 7 illustrates the photoactivity of the as-deposited Au-buffered TiO_2 thin film after its repeated use. It can be seen in Fig. 7 that the photocatalytic activity of the produced photocatalyst is not reduced after its repeated use.

4. Conclusion

We have investigated the photocatalytic activity of the Au-buffered TiO_2 thin films prepared by RF magnetron sputtering method. The photocatalytic activity of the amorphous Au-buffered TiO_2 thin films was superior to that of the pure anatase TiO_2 thin films because the Au-buffer layer may inhibit the charge carrier recombination by electron capture. As a result, more holes are available to produce hydroxyl radicals, thus enhancing the photodegradation. The surface area and anatase crystalline size of the Au-buffered TiO_2 films was increased post-annealing at 600 °C enhancing photocatalytic efficiency.

Acknowledgement

This work was supported by Korea Research Foundation Grant funded by the Korean Government (MOREHRD) (KRF-2006-521-C00067).

References

[1] M.R. Hoffmann, S.T. Martin, W. Choi, D.W. Bahnemann, Chem. Rev. 95 (1995) 69–96.
[2] Y. Ohko, A. Fujishima, K. Hashimoto, J. Phys. Chem. B 102 (1998) 1724–1729.
[3] J.M. Herrmann, Catal. Today 53 (1999) 115–129.
[4] S. Sakthivel, B. Neppolian, B. Arabindoo, M. Palanichamy, V. Murugesan, Indian J. Sci. Ind. Res. 59 (2000) 556–562.
[5] S. Sakthivel, M.V. Shankar, M. Palanichamy, B. Arabindoo, D.W. Bahnemann, V. Murugesan, Water Res. 38 (2004) 3001–3008.
[6] R. Comparelli, E. Fanizza, M.L. Curri, P.D. Cozzoli, G. Mascolo, R. Passino, A. Agostiano, Appl. Catal. B: Environ. 55 (2005) 81–91.
[7] L.K. Adams, D.Y. Lyon, P.J.J. Alvarez, Water Res. 40 (2006) 3527–3532.
[8] M.-S. Wong, W.-C. Chu, D.-S. Sun, H.-S. Huang, J.-H. Chen, P.-J. Tsai, N.-T. Lin, M.-S. Yu, S.-F. Hsu, S.-L. Wang, H.-H. Chang, Appl. Environ. Microbiol. 72 (2006) 6111–6116.
[9] Z.X. Lu, L. Zhou, Z.L. Zhang, W.L. Shi, Z.X. Xie, H.Y. Xie, D.W. Pang, P. Shen, Langmuir 19 (2003) 8765–8768.
[10] G. Gogniat, M. Thyssen, M. Denis, C. Pulgarin, S. Dukan, FEMS Microbiol. Lett. 258 (2006) 18–24.
[11] H. Haick, Y. Paz, J. Phys. Chem. B 107 (2003) 2319–2326.
[12] G. Fu, P.S. Vary, C.T. Lin, J. Phys. Chem. B 109 (2005) 8889–8898.
[13] I.M. Arabatzis, T. Stergiopoulos, D. Andreeva, S. Kitova, S.G. Neophytides, P. Falaras, J. Catal. 220 (2003) 127–135.
[14] F. Pan, J. Zhang, W. Zhang, T. Wang, C. Cai, Appl. Phys. Lett. 90 (2007) 122114–122116.
[15] L. Armelao, D. Barreca, G. Bottaro, A. Gasparotto, C. Maccato, C. Maragno, E. Tondello, U.L. Stangar, M. Berhant, Nanotechnology 18 (2007) 375709–375715.
[16] J.M. Jung, M. Wang, E.J. Kim, S.H. Hahn, Vacuum 82 (2008) 827–832.
[17] X.Z. Li, F.B. Li, Environ. Sci. Technol. 35 (2001) 2381–2387.
[18] S.Y. Zhao, S.H. Chen, S.Y. Wang, Z.L. Quan, J. Colloid Interface Sci. 221 (2000) 161–165.
[19] R. Zanella, S. Giorgio, C.H. Shin, C.R. Henry, C. Louis, J. Catal. 222 (2004) 357–367.
[20] H. Gerischer, A. Heller, Phys. Chern. 95 (1991) 5261–5267.
[21] A.L. Linsebigler, G. Lu, T. Yates, Chern. Rev. 95 (1995) 735–758.
[22] G. Tian, L. Dong, C. Wei, J. Huang, H. He, J. Shao, Opt. Mater. 28 (2006) 1058–1063.